14p

NASA TECHNICAL TRANSLATION NASA TT F-14,745

A STUDY OF CORONAL CONDENSATIONS BY MEANS OF THEIR X-UV LINE SPECTRUM

G. Chambe

(NASA-TT-F-14745) A STUDY OF CORONAL CONDENSATIONS BY MEANS OF THEIR X-UV LINE SPECTRUM (Techtran Corp., Silver Spring, Md.) ~~19~~ 20 p HC $4.00 CSCL 17E

N74-22319

G3/23 Unclas 37543

Translation of "Etude des condensations coronales a l'aide de leur spectre de raies X-UV," Astronomy and Astrophysics, Vol. 12, 1971, 9 pages.

NATIONAL AERONAUTICS AND SPACE ADMINISTRATION
WASHINGTON, D.C. 20546 AUGUST 1973

GSFC-94

STANDARD TITLE PAGE

1. Report No. NASA TT F-~~15,951~~ 14,745	2. Government Accession No.	3. Recipient's Catalog No.
4. Title and Subtitle A STUDY OF CORONAL CONDENSATIONS BY MEANS OF THEIR X-UV LINE SPECTRUM		5. Report Date April 1973 6. Performing Organization Code
7. Author(s) G. Chambe		8. Performing Organization Report No. 10. Work Unit No.
9. Performing Organization Name and Address Techtran Corporation P.O. Box 645, Silver Spring, Md. 20901		11. Contract or Grant No. NASw-2485 13. Type of Report and Period Covered Translation
12. Sponsoring Agency Name and Address NATIONAL AERONAUTICS AND SPACE ADMINISTRATION WASHINGTON, D.C. 20546		14. Sponsoring Agency Code

15. Supplementary Notes

Translation of: "Etude des condensations coronales a l'aide de leur spectre de raies X-UV," Astronomy and Astrophysics, Vol. 12, 1971, 9 pages.

16. Abstract: An interpretation of the X-UV resonance line spectrum of coronal condensations is given in terms of thermal emission from non-homogeneous regions, i.e., with a continuous range of temperatures.

It is shown that the temperature and the emission measure N_e^2V derived from the measured intensities of two lines depend on the pair of lines in such a way that an isothermal model cannot account for wide ionization and excitation potential ranges. In addition, the formation temperature domain of each line is not fine enough for us to neglect the variations of emission measures inside it. Therefore Pottasch's approximate method, valid for a quiet corona, is not suited for centers of activity. In the latter case, rigorous treatment is required.

We have adapted this calculation for the observed intensities of the Fe. XV, XVI, lines at ≈ 300Å, the Si VIII to XII lines in the 40-70Å band, and the O VII, VIII, Ne IX, X and Fe XVII, XVIII lines between 10 and 25Å.

Continued on next page...

17. Key Words (Selected by Author(s))	18. Distribution Statement		
Sun, X-UV line emission, coronal condensation: microwave and X radiation, density and temperature structures, element abundances	Unclassified-unlimited		
19. Security Classif. (of this report)	20. Security Classif. (of this page)	21. No. of Pages	22. Price
Unclassified	Unclassified	20	4.00

As there are no simultaneous observations for these spectral ranges, we used microwave data to select a set of X-UV spectra corresponding to similar solar conditions. We believe that this example is typical of teh case when two or three rather small condensations are present. The corresponding emission measure curve
measure curve $f(T) = d/dT \int N_e^2 \, dV$, is found to be of exponential form above $2 \cdot 10^6$°K:

$$f(T) \sim 10^{-T/T_0}, \text{ with } T_0 = 1.5 \cdot 10^6 \text{°K}$$

Maximum temperature ranged from 4 to 6 10^6°K.

The relative abundance of the elements is in good agreement with Pottasch's determination for a quiet corona, but absolute values twice as high are preferable to fit the radio data.

If there is no spatial resolution or inclusion of forbidden lines, the X-UV analysis cannot be carried further. It is shown that microwave data provide little more information for this kind of optically thin small condensations. Therefore, we used previous determinations of N_e and photographs of the Sun in wide X-UV bands, along with the f(T) function, to build a two--components model of coronal condensations: The first is a "facular region," about five feet wide, with $T_{max} \approx 2.5 \cdot 10^6$; the second is a "central core" of one foot size in which $T_{max} \geq 4 \cdot 10^6$. The temperature versus height curves are drawn for each component. The "transition zone" is found to be about 10^3 km thick, or less, with a tendency to lie at a lower altitude in the central region.

A STUDY OF CORONAL CONDENSATIONS BY MEANS OF THEIR X-UV LINE SPECTRUM

G. Chambe

I. INTRODUCTION

In the absence of eruption solar X-UV radiation is emitted by the corona /210* and the corona-chromosphere transition zone with reinforcements in the densest and hottest zones (coronal condensations), where contrast with the calm atmosphere is greater depending upon observation of the flux in a finer spectrum band or in a line with a higher excitation potential.

These results, predicted by theory (Elwert, 1961), have been confirmed by experiments of several types: simple measurements of total solar flux in different spectrum bands (Michard and Ribes, 1967); weak x-ray photographs (Underwood and Muney, 1967; Reidy et al., 1968) and spectroheliograms in the UV lines (Austin et al., 1966); spectra showing the lines of greatly ionized elements (Evans and Pounds, 1968).

The latter data are richest in information. This is why Neupert (1967), Evans and Pounds (1968), Beigman and Vainshtein (1970) made use of these spectra by proposing isothermal or quasi-isothermal models of coronal condensations. But we shall see that this limitation does not allow them to be satisfactory except inside rather restricted spectral domains.

Pottasch (1964 and 1967) published a method of analysis leading to a con- /211 tinuous distribution of atmosphere as a function of temperature. However, we shall show that for $T > 2 \cdot 10^6$ °K, i.e., roughly within centers of activity, certain of the approximations carried out are no longer valid. Therefore, it will be necessary to perform a rigorous calculation to extend this distribution into the high temperature range.

---

*Numbers in margin indicated foreign text pagination.

The procedure followed by Pottasch does not allow the models of density and temperature to be separated without introducing an additional hypothesis. This hypothesis is $P_c = N_c = T_c$ = constant in the works of Athay (1966), and of Dupree and Goldberg (1967) relating to a calm atmosphere. But this statement is not "self-consistent" (Delache, 1967; Pottasch, 1968) and its extension to condensations is difficult. This is why we propose to have recourse to observation data on density in order to obtain a temperature model.

The method used allows calculation of relative abundances, on the condition that they are presumed to be constant, a hypothesis which disagrees with the theoretical results of Delache (1967) and Nakada (1969), but which is acceptable in the light of recent revision of solar abundances.

As far as absolute abundances are concerned, they remain undetermined. The use of radio electrical data furnishes an additional equation, but introduces a new parameter, the magnetic field, which cannot be completely disregarded. At the end we shall make a comparison of our models with those of radio astronomers.

II. FORMULATION OF THE PROBLEM AND TRADITIONAL METHODS OF ANALYSIS

The theoretical intensity of a resonance line in the X domain on Earth (Pottasch, 1964) is

$$E = 7{,}8 \times 10^{-42}\, g f A_z \int N_e^2 G(T)\, dV \text{ erg cm}^{-2}\text{ s}^{-1} \qquad (1)$$

with

$$G(T) = T^{-1/2} e^{-w/kT} \frac{N_i}{N_z}$$

where N_i/N_z is the abundance of ion i of element z relative to this element, $A_z = N_z/N_H$ is its abundance relative to hydrogen. W is the excitation potential of the line (in eV). f, oscillator strength, is noted in Table 1, column three. g is a mean gaunt factor calculated according to Burgess (1964). It is close to 0.3 if $W/kT > 1$, i.e., for all the lines of Table 1 except for Fe XV and XVI for 300 Å, for which it is around 0.7.

We used the results of Bely (1967) for iron and of Allen and Dupree (1967) for the other elements for ionization equilibrium. Their calculations take into consideration dielectronic recombination and autoionization.

The establishment of equation (1) presumes that the population of the excited level is the result of electronic collisions on atoms in the ground state, while any other phenomenon, such as population by recombination or cascades, can be disregarded. This approximation is not valid for Fe XVII: as a matter of fact, Bely (1967b) has shown that cascades play a large part in the population of 3s levels. Following Evans and Pounds, we shall take this into consideration by multiplying the second member of (1) by three for lines 2p–3s (17.05 Å and 16.77 Å).

Equation (1) is generally used with one of the following hypotheses:

a) the emission source is isothermal,

b) each line is formed within a narrow temperature range.

We shall examine the validity of these approximations quantitatively.

1. Isothermal Source of Emission

This is the hypothesis made by Widing and Sandlin (1968), Neupert (1967) and, to a certain extent, by Evans and Pounds (1968) and by Beigman and Vainshtein (1970). The temperature is found by making a ratio of the measured intensities of two lines from the same element. According to (1):

$$\frac{E_1}{E_2} = \frac{g_1 f_1}{g_2 f_2} \frac{G_1(T)}{G_2(T)}.$$

Then, the "dimension" corresponding to the emissive region N_e^2V is furnished by the absolute intensity of a line. This method of analysis will be valid to the extent that T and N_e^2V do not depend on the pair of lines used. Now, in Evans and Pounds' interpretation of the spectrum obtained by them, the use of the lines of Ne IX and Ne X lead to $T = 3 \cdot 10^6$ °K and $N_e^2V = 1.7 \cdot 10^{48}\ cm^{-3}$, while consideration of Fe XVII and XVIII forces the addition of a hotter section to the emission source, e.g., an excess of 6% to $4 \cdot 10^6$ °K. The lines of Fe XV and XVI have been observed by Neupert who had deduced from the temperatures of $3.8 \cdot 10^6$ °K for an active region in formation and of $2.9 \cdot 10^6$ °K for an old band[1], and /212

[1]The calculations of ionization equilibria used by Neupert do not take autoionization into consideration. The temperatures found with Bely's calculations would be lower: 2.8 and $2.1 \cdot 10^6$ °K, respectively.

a value of N_e^2V of $2.3 \cdot 10^{49}$ cm^{-3}, far higher than the estimate of Evans and Pounds.

Therefore, since T and N_e^2V dependegreatly on the pair of lines used, it is clear that a model of continuous temperature distribution cannot be avoided.

TABLE 1. OBSERVATION DATA FOR THE X-UV LINE STUDY

ion	λ (Å)	f	flux mesurés (erg cm⁻² s⁻¹)							
			23/8/61		9/3/62		10/5/63		13/12/63	
Fe xv	284,3	0,82	31	10^{-3}	5,2	10^{-3}	17,2	10^{-3}	5,6	10^{-3}
Fe xvi	361,7	0,13	12	10^{-3}			5,0	10^{-3}	2	10^{-3}
	336,6	0,27	20	10^{-3}	5,8	10^{-3}	8,0	10^{-3}	4,1	10^{-3}
			2/9/63		3/11/65					
Si viii	61,0	1,18	4,3	10^{-3}	2,49	10^{-3}				
Si ix	55,4	0,71	10,3	10^{-3}	2,74	10^{-3}				
Si x	50,7	0,55	12,8	10^{-3}	3,45	10^{-3}				
Si xi	43,7	0,61	2,1	10^{-3}	(0,9)	10^{-3}				
Si xii	40,9	0,33	1	10^{-3}	(0,6)	10^{-3}				
			5/5/66						22/66/12	
			(1)		(2)		Total			
Fe xvii	17,05	0,11	84	10^{-5}	32	10^{-5}	116	10^{-5}	118	10^{-5}
	16,77	0,10	32	10^{-5}	13	10^{-5}	45	10^{-5}	74	10^{-5}
	15,45	0,01	22	10^{-5}	10	10^{-5}	32	10^{-5}	21	10^{-5}
	15,26	0,64	48	10^{-5}	18,5	10^{-5}	66,5	10^{-5}	56,5	10^{-5}
	15,01	2,24	74	10^{-5}	27,5	10^{-5}	101,5	10^{-5}	92,5	10^{-5}
	12,26	0,37	2,5	10^{-5}	1,2	10^{-5}	3,7	10^{-5}	8	10^{-5}
	12,12	0,41	2,8	10^{-5}	1,2	10^{-5}	4	10^{-5}		
Fe xvii	total						368,7	10^{-5}	370	10^{-5}
Fe xviii	14,40	1,90					4,5	10^{-5}	8	10^{-5}
	14,25	3,11					2,7	10^{-5}	14,4	10^{-5}
O vii	21,60	0,69					363	10^{-5}	141	10^{-5}
	18,63	0,15					56	10^{-5}	38	10^{-5}
	17,77	0,07					18	10^{-5}	7	10^{-5}
O viii	18,97	0,42	130	10^{-5}	54	10^{-5}	184	10^{-5}	174	10^{-5}
	16,01	0,08	20	10^{-5}	10	10^{-5}	30	10^{-5}	23	10^{-5}
	15,17	0,03	12	10^{-5}	7	10^{-5}	19	10^{-5}		
	14,82	0,01					2,2	10^{-5}		
Ne ix	13,45	0,72	18	10^{-5}	7,8	10^{-5}	25,8	10^{-5}		
	11,56	0,15	2,3	10^{-5}	1,0	10^{-5}	3,3	10^{-5}	5	10^{-5}
Ne x	12,13	0,42	1,7	10^{-5}	0,7	10^{-5}	2,4	10^{-5}	13	10^{-5}

Identifications of Wavelengths and Oscillator Forces are Those Used by Pottasch (1967) for Fe XV and XVI by Widing and Sandlin (1968) for Si, and by Evans and Pounds (1968) for the Other Lines.

References for the Observations: 23/8/61; 9/3/62 and 12/12/63: Hall et al. (1965). 10/5/63 and 20/9/63: Austin et al. (1966). 3/11/65: Manson (1967). 5/5/66: Evans and Pounds (1968). 22/12/66: Walker and Rugge (1968).

2. Approximation Method With G(T)

When the function G(T) is narrow, it can be replaced by a gap of width ΔT, of height $\{G(T)\}$ (Pottasch, 1964) with (1) being written in the form:

$$E = 7{,}8 \times 10^{-43} g f A_z \langle G(T) \rangle \int_{\Delta T} N_e^2 dV . \qquad (2)$$

The distribution curve of matter is obtained as a function of T by applying as the abscissa on a graph for each line the temperature at which G(T) is maximum, and as ordinate the quantity $A_z \int_{\Delta T} N_e^2 dV$ deduced from (2). Then the question is to find out if ΔT is sufficiently small for the variations of $\int N_e^2 dV$ in it to be disregarded. This is actually for the majority of lines formed around $1.6 \cdot 10^6$ °K, therefore in a calm corona, but it remains doubtful for coronal condensation, partly because the ionization equilibria curves broaden toward high temperatures and partly because of the great variations in /213
$\int N_e^2 dV$ suggested by the discussion in the previous paragraph.

We can represent the error committed by the difference between the temperatures of the maxima of the functions G(T) and dE/dT. This function dE/dT is calculated according to (1) by using what we eventually found to be the best model. The calculation shows that the difference increases from $0.1\text{-}0.3 \cdot 10^6$ °K for Si X-XII and Fe XV and XVI to $0.5\text{-}1 \cdot 10^6$ °K for O VII and VIII, and to $\approx 2 \cdot 10^6$ °K for Fe XVII and XVIII and for Ne IX and X, the direction being one of overestimation of the temperature from Pottasch's method.

To sum up, we shall say that it is necessary:

a) to make a strict calculation on the basis of a continuous temperature distribution,

b) to use lines allowing a large gamut of temperatures to be explored. Unfortunately, we do not have available simultaneous data for all of the spectrum domain which would permit such exploration. Therefore a sampling must be made from comparable observations.

III. OBSERVATION DATA

The spectral zones for which we have the best observations available are situated near 10-25 Å, 40-70 Å and around 300 Å. We have chosen the intense lines of these domains and noted the fluxes measured in the columns from four on

in Table 1. This concerns global solar fluxes, because the experiments do not have any spatial resolution, except for 5-5-66 where Evans and Pounds were able to separate two condensations of the coronal background: the corresponding fluxes are found under numbers (1) and (2) in Table 1.

Nevertheless, a separation of the totality of condensations is possible because they are 100% responsible for the flux for Ne IX, X, Fe XVII, XVIII and of the major part (80%) for O VIII, Fe XV, XVI, (Evans and Pounds, 1968; Neupert, 1967), with their contribution becoming weaker for O VII and for silicon, decreasing with the degree of ionization. Despite all the this the corresponding lines are usable for evaluating the dimensions of condensation in relation to those of a calm corona.

Since the X-UV condensation emissions vary greatly from one day to another, it is not possible to extract a "mean" observation from them. It is better to select dates corresponding to comparable solar situations based on the correlation found between X and radio centimeter radiation from the centers of activity (Michard and Ribes, 1967; Neupert, 1967).

Figure 1 shows the spectra obtained by making on a given day a summary of the fluxes emitted by the different acitve regions visible on the radio electrical maps of Sidney (21 cm) and Stanford (9.1 cm) and on the 3 cm recordings of Nancay. It is obvious that the situations corresponding to 10-5-63 (300 Å experiment) and to 5-5-66 and 22-12-66 (10-25 Å) are similar. The global fluxes measured on the two latter dates are likewise close, except for the higher ionization states (Fe XVIII and Ne X). We shall take the measurements of 10-5-63 and 5-5-66 as "base data" to be reproduced in theory. On the other hand, Figure 1 shows 40-70 Å domain that the silicon line intensities measured on 20-9-63 and 3-11-65 cannot be considered except as upper and lower limits.

IV. DISTRIBUTION OF MATTER AS A FUNCTION OF TEMPERATURE

We begin by examining the distribution corresponding to all of the solar atmosphere visible from Earth. Such a distribution can be expressed as: /214

$$f(T) = \frac{d}{dT} \int N_e^2 dV \qquad (3)$$

and represents the portion of $\int N_e^2 dV$ associated with each temperature. The

method consists of choosing *a priori* f(T) for which the intensities of the lines calculated by equation:

$$E = 7{,}8\,10^{-8} g f A_z \int f(T) G(T) dT \qquad (4)$$

agree with the measured values. The function f(T) should have "regular variations" and only its slope is significant since A_z is not determined. Therefore, the conditions of the problem are: a) that the various elements can be associated with one and the same function f(T) with an approximate multiplying factor, b) that the relative abundances furnished by these factors do not differ very much from values previously found.

Results. The distribution $f_1(T)$ providing the best agreement with the "basic data" is shown in Figure 2. Above $2 \cdot 10^6$ °K it has an exponential shape: $f_1(T) \sim \sim 10^{-T/T_e}$, with $T_0 = 1.5 \cdot 10^6$ °K. The absolute value $f_1(2 \cdot 10^6\ °K) = 10^{49}$ cm^{-3} $(10^6 \cdot °K)^{-1}$ is obtained by making the estimate $A_{Fe} = 65 \cdot 10^{-6}$, which is the best for the corona according to Pottasch (1964b) and Jordan (1966).

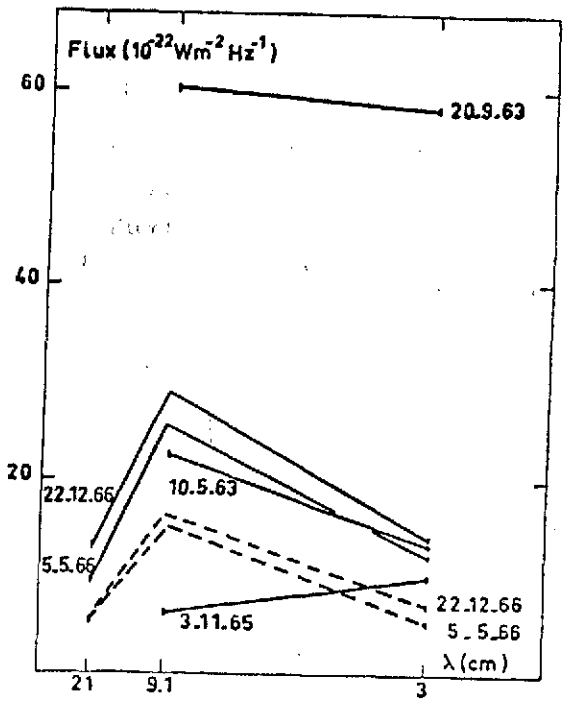

Figure 1. Radioelectrical Spectra of All Visible Condensations For Different Dates (Solid Lines). The spectrum of the greatest condensation on 5-5-66 and 22-12-66 has also been shown (dotted lines).

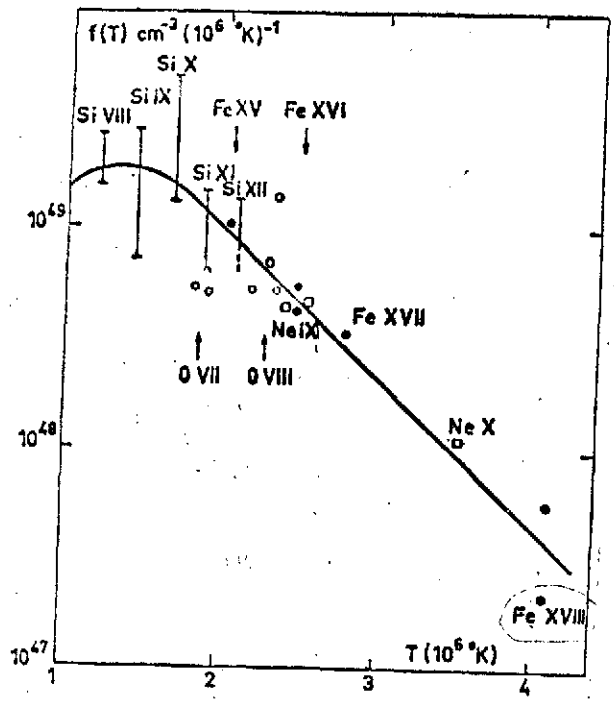

Figure 2. Distribution $f_1(T)$ Relative to the Entire Corona and its Condensations. The points correspond to different lines: their abscissa is the temperature at which dE/dT is maximum and their ordinate = f_1 (T) × E (experimental)/E (calculated). ○O, □Ne, I Si ○Fe.

The difference between the theoretical and the given values can be seen in Figure 2 where, for each line, the abscissa includes the temperature providing $dE/dT \sim f_1(T)G(T)$ maximum and the ordinate has the quantity $f_1(T) \times E$ (experimental)/E(calculated). A single point corresponding to all the lines represents Fe XVII to avoid a large dispersion due to theoretical difficulties mentioned in section II. The Fe XV to XVII ions best assure determination of f(T) since their lines are scales from $2\text{-}4 \cdot 10^6$ °K. Agreement is excellent for neon. On the other hand, the most noticeable dispersion for oxygen may originate in experimental causes, since the lines of O VII are situated at the edge of Evans and Pounds' observation window. The environment desired for silicon provided by the data from 20-9-63 and 3-11-65 is achieved by referring $f_1(T)$ to low temperatures, which is compatible with the distribution found by Pottasch (1967) with a large number of lines and represented in Figure 3 (curve P).

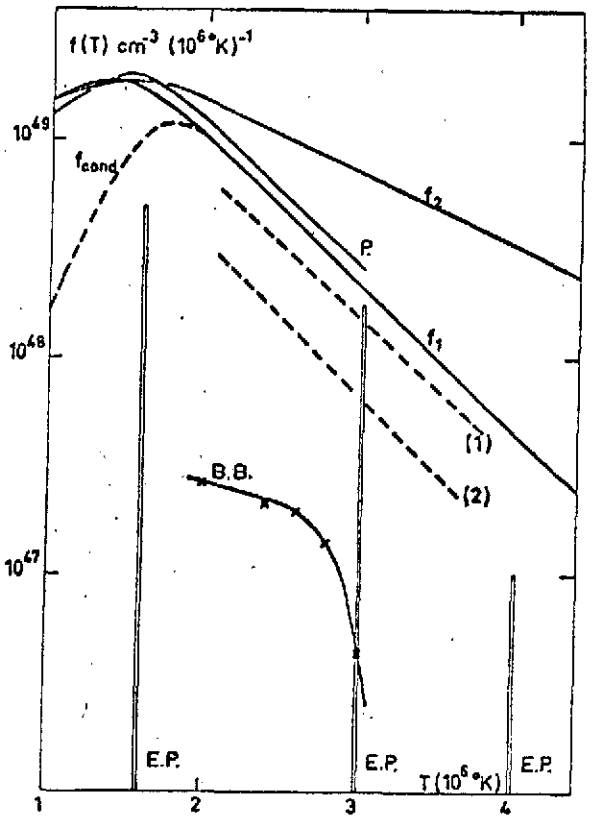

Figure 3. Comparisons of Distributions f_1 and f_2 With Those of Pottasch, 1967 (P), Boardman and Billings, 1969, (B. B.) and Evans and Pounds, 1968 (E. P.: Line Height Calculated for a "Width Equivalent" to 16^6 °K). (1) and (2) are the distributions associated with each of the two condensations visible on 5-5-66, the sum of which make f_{cond}.

The theoretical values used to determine Figure 2 were calculated by cutting $f_1(T)$ at $4 \cdot 10^6$ °K. The choice of a higher temperature would change the intensities only for the lines of Fe XVIII and Ne X. This is why the experiment of Walker and Rugge on 22-12-66 can be associated with the same distribution but extended up to $6 \cdot 10^6$ °K. As far as the strong intensities measured on 23-8-21 and 20-9-63 for Fe XV, XVI and Si VIII-XII, these can be interpreted with the distribution $f_2(T)$ shown in Figure 3, with behavior in $10^{-T/T_e}$, for $T > 2 \cdot 10^6$ °K, with $T_0 = 3 \cdot 10^6$ °K and $f_2(2 \cdot 10^6 \text{ °K}) = 1.5 \cdot 10^{49}$. The intensities

of the lines in the 10-20 Å domain predicted in this way are several times greater than the base data, which is compatible with the dynamics of the slowly variable component in the spectral zones (Michard and Ribes, 1967).

Separation of the Various Atmospheric Components

This is a delicate problem. But according to the discussion in Section II on the distribution of the flux of each line, it can be said that: for $T > 2 \cdot 10^6$ °K, the function $f_1(T)$ of Figure 2 is equal to the distribution $f_{cond}(T)$ in single condensation; on the other hand, above $1.5 \cdot 10^6$ °K, coronal contribution is /215 greater. The determination of $f_{cond}(T < 2 \cdot 10^6)$, essential for identifying the temperature gradients at the basis of the condensations, will only be realized when the spectra of isolated active regions have been measured by a collimator. Based on the estimate that the active regions occupy 2.5% of the visible disc with a density twice as great as the corona at 10^6 °K, we get $f_{cond}(10^6) \approx 1/10\ f_1(10^6)$. This permits us to trace a hypothetical representation of $f_{cond}(T)$ in Figure 3, which we shall use later. In this figure curves (1) and (2) represent the contributions of each of the condensations separated by Evans and Pounds, the sum of which forms f(T).

For the sake of comparison we have also represented the two-temperature model proposed by Evans and Pounds for condensation (1) (identified as E. P. in Figure 3). The same group has recently obtained new spectra between 3 and 15 Å of several condensations (Batstone et al., 1970) and has interpreted them in terms of flatter distributions than ours and extended up to $9.5 \cdot 10^6$ °K.

V. MODELS OF CORONAL CONDENSATIONS

In the absence of a sufficient separating power, we cannot provide a three-dimensional model. At first T and N_e are presumed to be a function of the variable of altitude h alone for the points situated above the surface S. Equation (3) is written:

$$\frac{dT}{dh} = \frac{SN_e^2}{f(T)} \tag{5}$$

where it is convenient to choose the determination $f_{cond}(T)$ for f(T), and the sum of the condensation areas for S.

Now, photographs, spectroheliograms and eclipse measurements (Simon, 1969) indicate that:

a) The sources photographed in the spectral bands of weak x-rays or in the UV lines, where the formation temperature is less than or equal to that of Fe XVI (i.e., $\leqslant 2.5 \cdot 10^6$ °K according to Figure 2), have dimensions on the order of several minutes.

b) The sources of finer x-ray emissions (λ . 20Å) have a diameter not exceeding one minute, which is consistent with the radio measurements at 3 cm (Kundu, 1964).

Therefore we shall distinguish two components in the model: one connected with facular regions (PF) where $T_{max} = 2.5 \cdot 10^6$ °K and where S is estimated at $.8 \cdot 10^2$ cm^2 (which corresponds, for example, to two condensations with PF of five minutes extension); the other made up of central cores (NC) characterized by $T_{max} \geqslant 4 \cdot 10^6$ and $S = 5 \cdot 10^{-9}$ cm^2 (equivalent to two cores of a diameter of one minute). The integration of (5) is carried out in each component. In order to extend the result relative to central cores below $2.5 \cdot 10^6$ °K, we have presumed that:

$$f_{NO}(T) = f_{cond}(T) \times \frac{(SN_e^2)_{NC}}{(SN_e^2)_{NC+PF}}.$$

This is integration is possible only by means of an additional equation between T, N_e and h: for example, the equation of hydrostatic equilibrium or of heat conducting flux constancy. However, such equations would not be realistic unless a model of a magnetic field were chosen. We prefer to get $N_6(h)$ directly by proceding from the models of Thomas and Athay (1961), Pagel (1964) /216 and van de Hulst (1953) for a calm corona (curve N_{eCC} shown in Figure 4) and by choosing values five and ten times greater in PF and NC, respectively. These factors are determined by finding agreement with the measurements of Newkirk (1961 and 1967) for coronal streamers.

The temperature models obtained are shown in Figure 4 (curves PF_1 and NC_1). From the various curves of the integrated network we have chosen those which reach maximum temperature around 40,000 km, which seems reasonable according

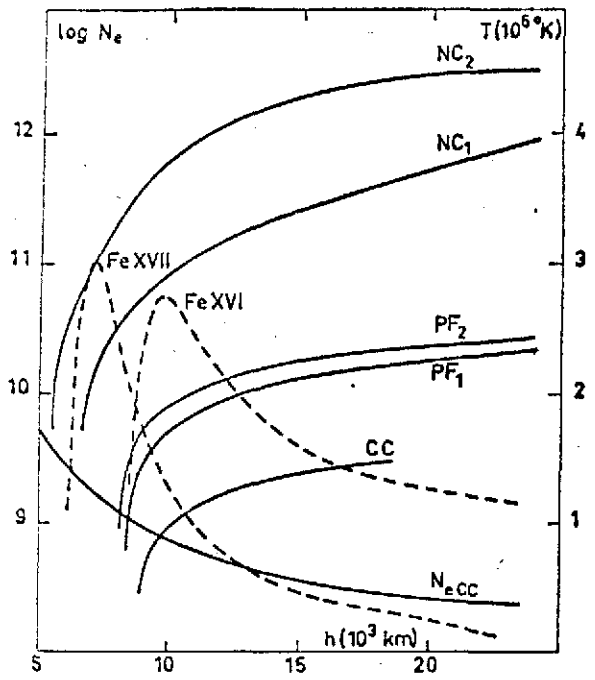

Figure 4. Temperature Models Obtained For a Calm Corona (CC) of "Facular Regions" (PF) or of "Central Cores" (NC). Indices 1 and 2 correspond to the choice of f_1 or f_2 (Figure 3). The dotted lines represent the emission profiles at the level of Fe XVI and Fe XVII in the case PF_1 + + NC_1 (arbitrary linear scale).

to the photographs of the limbus and eclipse measurements. In addition, the position and the rigidity of the transition zone are quite insensitive to the height assigned to T_{max}.

For comparison we have also traced the temperature model for a calm corona (CC) obtained by taking our distribution $f_1(T)$ between 10^6 and $1.5\cdot10^6$ °K extended by Pottasch's distribution (1967) to lower temperatures, and with $S = 2\pi R_\odot^2$ (visible semi-corona). The dotted curves PF_2 and NC_2 correspond to the choice of distribution $f_2(T)$ indicating greater solar activity.

When the sources are classified according to spectra of increasing fineness: CC, PF, PF_2, NC_1, NC_2, it is found that the same temperatures are obtained at lower and lower points with higher gradients. However, these displacements may be partially caused by variations in the choice of the parameters.

In order to clarify this point, let us write (5) in the form:

$$\frac{dT}{dh} = \frac{SN_e^2(h)A_z}{A_z f(T)}$$

making the quantity $A_z f(T)$, the only one determined by the X-UV analysis, stand out. Discussion is reduced to studying the influence of the single parameter

$$\alpha = SN_e^2(h)A_z/(SN_e^2(h)A_z)_0$$

where the zero index designates the values previously chosen. Calculation shows that the choice $\alpha = 2$ ($\alpha = 1/2$) raises (lowers) the transition zone by about 1,000 km.

We have not paid any attention to the upper part of the condensation where $dT/dH < 0$. After a study similar to ours, Landini and Monsignori Fossi (1970) proposed a model with a semi-spherical geometry where the temperature is lower on the exterior hemispheres. Boardman and Billings (1969) also go in this direction: after observing on the east edge of a UV spectroheliogram on 28-5-66 one of the condensations studied several days later by Evans and Pounds, they provided isodensity and isotemperature curves indicating a decrease of from $3\text{-}1 \cdot 10^6$ °K in 40,000 km. However, the distribution f(T) deduced from these curves and represented in Figure 3 (curve B. B.), is well below $f_1(T)$, indicating that the source of emission is concentrated at the base. In our PF_1 + NC_1 model the emission profiles $dE/dh \sim N_2^e G(T)$, designed for Fe XVI and XVII in Figure 4, clearly show a concentration toward 10,000 km altitude associated with a diffuse section extending over several tens of thousands of kilometers.

VI. RADIOELECTRIC EMISSION FROM CORONAL CONDENSATIONS

1. General Considerations

We test our models by radioelectrical emission in the case of the greatest condensation observed on 5-5-66, the spectrum of which between 3 and 21 cm is shown in Figure 2, and the material distribution of which can be evaluated at 2/3 $f_1(T)$ (Figure 4). The magnetic field is disregarded, which is justified at 21 cm but not entirely so at 9.1 cm. The calculation would have most significance at higher frequencies in the absence of a magnetic field model. /216

The free-free absorption coefficient is

$$\varkappa_\nu = \frac{\xi N_e^2}{\nu^2 \mu T^{3/2}}$$

where ξ is a slowly variable function of T and ν amounting to 0.16 in the corona and 0.11 in the chromosphere.

$$\mu^2 = 1 - f_0^2/\nu^2 ; \quad f_0 = 9\,10^3 N_e^{1/2}$$

being plasma frequency. In our models μ remains close to one, except for a central core at 21 cm and for a choice of high density.

Before carrying out the calculation, let us try to define the additional information we may hope to obtain. With the help of (5) we can write the optical density $\tau_\nu = \int_{h_1}^{h_2} \chi_\nu dh$ in the shape:

$$\tau_\nu = \frac{1}{\nu^2 S} \int_{T_1}^{T_2} \frac{\xi f(T)}{\mu T^{3/2}} dT$$

an expression which scarcely depends on the density if μ varies little. The brilliancy temperature is:

$$T_B = \int T e^{-\tau} d\tau = \frac{1}{\nu^2 S} \int e^{-\tau} \frac{\xi f(T)}{\mu T^{1/2}} dT$$

and the fluxes emitted by the region of area S:

$$I = 3{,}07 \frac{S}{R^2} \nu^2 T_B \, 10^{-40} \, \mathrm{W m^{-2} Hz^{-1}}$$

where R = 1 AU. This finally provides:

$$I = 1{,}35 \times 10^{-44} \int \frac{e^{-\tau}}{\mu} \frac{\xi f(T)}{T^{1/2}} dT . \qquad (6)$$

As long as τ remains small, this expression is independent of τ and therefore of ν, a well-known result, and especially of S. Now, one of the results of rigorous calculation will be that the greater part of the radiation comes into being in the facular region above the level T = 10^6 °K, a layer which is necessarily optically thin because the brilliancy temperatures observed are clearly lower.

The consequence of this is that, for a given function f(T), the radioelectrical flux is not very sensitive to a particular choice of models defined by S and $N_e^2(h)$. The only factor subject to discussion is the abundance of the elements which comes into play through the mediation of f(T). Naturally, this is not necessarily valid for the central core (but radiotelescopes have a

resolution power which is too weak to study it separately) nor for the greater condensations where the optical density can be quite large.

2. Emission at 21 cm and 9.1 cm

We carried out a rigorous calculation using equation (6) and the model (PF_1 + NC_1) of Figure 4 in order to check on the variations of μ. By retaining the abundance of Table 2, we obtain a flux of 11.2 (in units of $10^{-22}\,Wm^{-2}Hz^{-1}$) at 21 cm and of 14.7 at 9.1 cm, while the fluxes measured are 5.5 and 15.2. Agreement is found only at 9.1 cm. With double abundancies (therefore with a distribution f(T) one-half less) the fluxes calculated are 6.5 and 8.3. This situation is to be preferred because agreement is found at 21 cm and the insufficient flux found at 9.1 cm is explained by the fact that the magnetic field (the effect of which is to increase emission) has been disregarded.

Therefore, the abundances of Table 2 could be too weak by a factor of two.

TABLE 2. ABUNDANCES BY RATIO TO HYDROGEN.

	In this analysis	Pottasch, 1967	Evans et Pounds, 1968	Photosphere
O	300	325	500	910
Ne	30	45,5	55	
Si	52	65		32
Fe	65	65	140	3,7

VII. CONCLUSIONS

The following points have been made in regard to coronal condensations:

a) The atmospheric distribution $f(T) = \frac{d}{dT}\int N_e^2 dv$ given by the study of the X-UV resonance lines should be extended up to $T \geqslant 4\cdot10^6\,°K$ and cannot be approached by an isothermal model. Because of the rapid variations of f(T), the preferred formation level of a line is not that where G(T) is maximum.

b) The relative abundancies found are close to those of Pottasch for a calm corona. But double absolute abundances are preferable to interpret the radioelectrical data.

c) It is not possible to separate density and temperature distributions. The radioelectrical data for the type of condensations studied (optically thin toward λ = 10 cm) provide little precision because the domain of useful frequencies is reduced as long as the magnetic field is not introduced and because the separating power of the instruments is insufficient. /218

d) With a choice of a two-component model: a "facular region" and a denser and hotter "central core," we can determine the variations of temperature with altitude. The transition zone **is found as a scale on the order of 1,000 km.** It is lower with higher temperaturesgradients in the central core than in the facular region.

Among the weak points of the analysis, we may stress the inexactitude of the determination of $f(T)$ for experimental reasons (incoherence of data, too small a number of lines measured, confusion between calm corona and condensations) and theoretical reasons (uncertainty about the oscillating forces, lack of knowledge of the exact importance of the different microscopic mechanisms and of the physical conditions of the environment).

Another difficulty is that comparison of the resonance lines does not provide any information about density. Jordan (1969) has shown that the ratio of intensity of forbidden lines and of intermingling of helium ions is sensitive to density. This has been applied by Batstone et al., (1970). Therefore we may hope that in the near future it will be possible to specify separate models for density and temperature.

Acknowledgments. We would like to thank R. Michard who has welcomed us into his team and provided the subject of this work, and Mr. Pick for his help and for the many suggestions he has made.

REFERENCES

Allen, J. W. and A. K. Dupree, *Scientific Report*, Harvard College Observatory, No. 24, 1969.

Athay, R. G., *Ap. J.*, Vol. 145, p. 784, 1966.

Austin, W. E., J. D. Purcell, R. Tousey and G. K. Widing, *Ap. J.*, Vol. 145, p. 373, 1966.

Batstone, R. M., K. Evans, J. H. Parkinson and K. Pounds, *Solar Phys.*, Vol. 13, p. 389, 1970.

Beigman, I. L. and L. A. Vainshtein, *Astr. Zu.*, Vol. 47, p. 1030, 1970.

Bely, O., *Ann. Astrophys.*, Vol. 30, p. 953.

Bely, O., *Solar Phys.*, Vol. 2, p. 285, 1967b.

Boardman, W. J. and D. E. Billings, *Ap. J.*, Vol. 156, p. 731, 1969.

Burgess, A., Reports Culham Symp. Atomic Collisions, p. 63, 1964.

Delache, P., *Ann. Astrophys.*, Vol. 30, p. 827, 1967.

Dupree, A. K. and L. Goldberg, *Solar Phys.*, Vol. 1, p. 229, 1967.

Elwert, G., *J. Geophys. Res.*, Vol. 66, p. 391, 1961.

Evans, K. and K. A. Pounds, *Ap. J.*, Vol. 152, p. 319, 1968.

Hall, L. A., W. Schweizer and H. E. Hinteregger, *J. Geophys. Res.*, Vol. 70, p. 2241, 1965.

Jordan, C., *Mon. Not. R. astr. Soc.*, Vol. 132, p. 515, 1966.

Jordan, C., *Mon. Not. R. astr. Soc.*, Vol. 145, p. 241, 1969.

Kundu, M. R., The University of Michigan Scientific Report No. 64-4, 1964: Solar Radio Astronomy, Vol. II.

Landini, M. and Monsignori B. C. Fossi, submitted to *Solar Phys.*, 1970.

Manson, J. E., *Ap. J.*, Vol. 147, p. 703, 1967.

Michard, R. and R. Ribes, Proceedings I.A.U. Symp. No. 35, Reidel, Dordrecht, p. 420, 1967.

Nakada, M. P., *Solar Phys.*, Vol. 7, p. 302, 1969.

Neupert, W. M., *Solar Phys.*, Vol. 2, p. 294, 1967.

Newkirk, G., I.A.U. Symp. On the Development of Solar Active Regions, Budapest, Hungary, 1967.

Pagel, B. E. J., *A. Rev. Astr. Astrophys.*, Vol. 2, p. 267, 1964.

Pottasch, S. R., *Space Sci. Rev.*, Vol. 3, p. 816.

Pottasch, S. R., *Mon. Not. R. Astr. Soc.*, Vol. 128, p. 73, 1964b.

Pottasch, S. R., *Bull. astr. Inst. Netherl.*, Vol. 19, p. 113, 1967.

Pottasch. S. R., *Ap. J.*, Vol. 150, p. 361, 1968.

Reidy, W. P., G. S. Vaiana, T. Zehnpfennig, and R. Giacconi, *Ap. J.*, Vol. 151, p. 333, 1968.

Simon, G., *Solar Phys.*, Vol. 5, p. 19, 1969.

Thomas, R. N. and R. G. Athay, Physics of the Solar Chromosphere, Interscience, New York, 1961.

Underwood, J. H. and W. S. Muney, *Solar Phys.*, Vol. 1, p. 129, 1967.

Van de Hulst, H. C., The Sun, Kuiper, Ed. Univ. of Chicago Press, Vol. I, II, Chap. 5, 1953.

Walker, A. B. C. and H. R. Rugge, *Solar Flares and Space Research*, North Holl., Amsterdam, p. 102, 1969.

Widing, K. G. and G. D. Sandlin, *Ap. J.*, Vol. 152, p. 545, 1968.

Gilbert Chambe
Observatoire de Meudon
Department Solaire
F-92 Meudon, France

Translated for the National Aeronautics and Space Administration under contract No. NASw-2485 by Techtran Corporation, P. O. Box 645, Silver Spring, Maryland, 20901.